Department of Aerospace Engineering

University of Cincinnati

EROSION IN RADIAL INFLOW TURBINES - VOLUME IV

EROSION RATES ON INTERNAL SURFACES

By:

W.B. Clevenger, Jr.

and

W. Tabakoff

Supported by:

NATIONAL AERONAUTICS AND SPACE ADMINISTRATION

Lewis Research Center

Contract NGR 36-004-055

NASA CR-134677

EROSION IN RADIAL INFLOW TURBINES - VOLUME IV

EROSION RATES ON INTERNAL SURFACES

By:

W.B. Clevenger, Jr.

and

W. Tabakoff

Supported by:

NATIONAL AERONAUTICS AND SPACE ADMINISTRATION

Lewis Research Center

Contract NGR 36-004-055

1. Report No.	2. Government Accession No.	3. Recipient's Catalog No.
NASA CR 134677		

4. Title and Subtitle	5. Report Date
Erosion in Radial Inflow Turbines - Volume IV Erosion Rates on Internal Surfaces	January 1975 6. Performing Organization Code

7. Author(s)	8. Performing Organization Report No.
W.B. Clevenger, Jr. and W. Tabakoff	

9. Performing Organization Name and Address	10. Work Unit No.
Department of Aerospace Engineering University of Cincinnati Cincinnati, Ohio 45221	11. Contract or Grant No. NGR 36-004-055

12. Sponsoring Agency Name and Address	13. Type of Report and Period Covered
National Aeronautics and Space Administration Washington, D.C. 20546	Contractor Report 14. Sponsoring Agency Code

15. Supplementary Notes

Final Report. Project Manager, Jeffrey E. Haas, Fluid Systems Components Division, NASA, Lewis Research Center, Cleveland, Ohio 44135

16. Abstract

An analytic study of the rate at which material is removed by ingested dust impinging on the internal surfaces of a typical radial inflow turbine is presented.

The study indicates that there are several regions which experience very severe erosion loss, and other regions that experience moderate levels of erosion loss.

The greatest amount of material loss occurs on the trailing edges of the nozzle blades where very high velocity, moderate angle impacts occur. In addition, the tip regions of ductile materials are also subjected to serious levels of erosion loss.

Moderate amounts of erosion occur near the end of the scroll and on a few of the nozzle blades near this location.

Results are presented in the form of surface contours that exist on the scroll and blade surfaces after continuous particulate ingestion with time.

17. Key Words (Suggested by Author(s))	18. Distribution Statement
Radial Turbine Erosion Similarity Particulated Flow	Unclassified - unlimited

19. Security Classif. (of this report)	20. Security Classif. (of this page)	21. No. of Pages	22. Price*
Unclassified	Unclassified	41	$3.00

* For sale by the National Technical Information Service, Springfield, Virginia 22151

TABLE OF CONTENTS

SUMMARY

An analytic study of the rate at which material is removed by ingested dust impinging on the internal surfaces of a typical radial inflow turbine is presented.

The study indicates that there are several regions which experience very severe erosion loss, and other regions that experience moderate levels of erosion loss.

The greatest amount of material loss occurs on the trailing edges of the nozzle blades where very high velocity, moderate angle impacts occur. In addition, the tip regions of ductile materials are also subjected to serious levels of erosion loss. The tip regions of harder, more brittle materials are shown to experience much less erosion damage.

Moderate amounts of erosion occur near the end of the scroll and on a few of the nozzle blades near this location. This occurs even though the velocities of particles in these regions tend to be relatively slow; and results from a concentration effect that causes all particles to impact a very small surface area.

Results are presented in the form of surface contours that exist on the scroll and blade surfaces after continuous particulate ingestion with time.

INTRODUCTION

Particle erosion in gas turbine engines has become important because significant decreases in the operating life and rated performance have resulted when these engines are used in dusty environments. For example, the engines in military helicopters, operating at low altitudes and remote landing fields, have significantly shorter life and a more rapid performance deterioration rate than engines operating from hard surfaced landing fields and at higher altitudes. Although these helicopters have main engines which utilize axial flow turbines, some also have auxiliary power sources for special devices which utilize radial turbines, as shown schematically in Figure 1. Radial inflow turbines have also been used on small portable power plants which are also likely to be used in areas where dust ingestion will occur. Radial inflow turbines also are seriously being considered for future use in advanced helicopter engines and transportation vehicles such as trucks, buses, and automobiles. These engines will at times have incomplete filtering of incoming air, leading to the ingestion of erosive-size particles that could seriously degrade engine performance.

The radial turbine engines have, however, a more serious erosion problem than axial-flow turbines. In radial turbines, the heavier particles can experience a radially outward centrifugal force that is greater than the radially inward component of the aerodynamic drag force. In the axial-flow turbine, the centrifugal force acts perpendicular to the aerodynamic drag force. Thus, in radial turbines the heavier particles can be trapped between the stator and rotor, resulting in the particles striking the trailing edges of the stators and the leading edges of the rotor many times. In axial-flow turbines, the particles generally move outward to the tip region, but all particles have a tendency to pass through the turbine.

As a result of the wide interest in using radial turbines and because erosion seems to be more severe in radial turbines, an investigation was sponsored by the NASA Lewis Research Center to study erosion phenomena in radial inflow turbines and to find

ways of eliminating this erosion. Included in this investigation are analytical studies of particle trajectories through a radial inflow turbine and predictions of the effect of blade materials erosion by the action of particles. The results of these investigations will be published in a series of five volumes.

Volumes I through III (1, 2, 3) have dealt with the concept of erosive particle trajectories and studied the approximate velocities and types of impacts that occurred on surfaces inside a radial turbine as particles moved through the turbine.

Volume III (3) indicated several possible problem areas within a radial turbine. The first is the region at the end of the scroll, where the more rapidly changing radius of curvature causes more moderate angle impacts by the particles. Because of the nature of the motion of particles in the scroll, those particles that do not immediately enter the stator will tend to accumulate and enter a few of the blade passages near the scroll exit. Volume III also revealed that most heavier particles will become trapped in the vortex region of the turbine and repeatedly strike the trailing edges of the stator and the rotor leading edge.

The purpose of this report (Vol. IV) is to review recent erosion data. This data will be extrapolated using analytically determined particle trajectories to predict erosion damage in a radial turbine. This study will show where the erosion damage problem areas are and provide a basis for the selection of materials that would be less likely to experience severe erosion damage.

The erosion effects from the continuous action of SAE Standard Fine Dust at various concentration levels will also be considered in this study. These concentration levels are identical to those used in Reference 4. This reference presented results for the action of erosive dust on a real gas turbine engine. The results provided in this reference will provide worthwhile comparisons of the results that are presented here.

Additional references that describe mechanisms of erosion will be cited and discussed in the following section.

REVIEW OF EROSION MECHANISMS

The primary emphasis of the research that has been described in the other volumes of this series of reports has been restricted to the trajectories that erosive particles follow in the several different types of flow fields within the radial inflow turbine. These studies provided information on the locations and the types of impacts that occur within the turbine. In order to predict erosion from this information, a review of recent theories on the mechanics of erosion was made, and these theories were then applied to predict the erosion rates of several surfaces within the radial turbine.

The mechanics of erosion are separated into general categories dealing with particle impingment on surfaces constructed of ductile materials, such as common turbine metals, and brittle materials, such as some very hard alloys and ceramics. The categories are further subdivided for particle striking the surface at moderate angles of incidence in the range from 10° to 45°, and at high angles of incidence corresponding to angles greater than 45°. For each erosion category the parameters that influence erosion rates will be considered analytically and compared to experimental results.

Ductile Erosion

The first subcategory for ductile erosion to be discussed is that of particle impact on the surface at moderate incidence angles. I. Finnie in references 5, 6 and 7 has done the most to study ductile erosion by collecting experimental data and by developing theoretical models. These theoretical models are generally accepted as most valid.

The theoretical model assumes that sharp edges of the particle act as a tool and cut into the surface material when the stress exerted by the impact of the particle exceeds the material's plastic flow stress. The chip of material cut away by the particle is the surface material lost by erosion.

Using this model, Finnie, in Reference 7, develops an equation that describes the erosion volume loss of the material. This expression is given by

$$Q = \frac{k_o \, f(\beta_i) \, m \, V_i^2}{p} \qquad (1)$$

where Q is the volume loss from the surface, (meter^3),
k_o is a constant for the specific erosion system,
$f(\beta_i)$ is a function of the incidence angle,
m is the dust particle's mass, (kilograms),
V_i is the dust particle's velocity, (meters/second),
p is the minimum flow stress of target material, at the test temperature, (Newtons/meter^2).

The experimental data accumulated in References 5, 6, and 7 as well as data accumulated by most other references cited here generally agree with the expression given in Equation (1).

It is worth noting that this expression relates the erosion rates to the kinetic energy of the particle and the inverse of the material's flow stress. The expression does not include material properties of the particle, but is generally thought to apply whenever the particle is harder than the surface material.

Previous work, reported in Reference 8, described the resistance to erosion of several materials with liquid flow in which particulate material is suspended. This work was done to investigate the effects of dirt particles on hydraulic turbines in hydroelectric power stations. The data on erosion resistance was compared in terms of the hardness of the materials. This data showed that the erosion resistance of a material decreases quickly as the hardness of the particle material exceeds the hardness of the surface material.

Equation (1) does not describe the erosion phenomenon at incidence angles greater than about 45°. Several authors have considered theoretical and empirical methods that would modify Equation (1) so that it could be used for incidence angles up to

90°. References 9, 10, and 11 all present various equations that could be used to describe erosion from 0 to 90° incidence angles. These authors define two types of wear. The first is wear due to cutting, as described in Equation (1), and the second is wear due to repeated deformation. This deformation wear is caused by the repeated blows suffered by the specimen and eventually causes cracking and spalling of the material. It is this deformation wear that accounts for the erosion when particles strike the surface at incidence angles of 90°.

The expressions that have been developed in References 9, 10, and 11 are results of erosion models that allow precise mathematical description of the erosion phenomena. In addition, however, the repeated deformation wear predicted by the theoretical model seems to be less than the amounts of erosion that actually occur. These results have led to another physical model of the erosion phenomena which is given in Reference 12. This work proposes several mechanisms which in combination lead to the erosion of the surface. These mechanisms include a roughening of the surface by plastic deformation caused by the impacting particle. This roughening of the surfaces causes the particles to impact local regions at more moderate angles, which can lead to erosion as predicted in Equation (1). In addition, the plastic deformation causes a battering of the surface which leads to local failure of the material by low cycle fatigue. Experimental evidence given in Reference 13 partially supports this theory, but more experimental evidence is needed before this theory can be accepted completely. No attempt was made in Reference 12 to develop a theoretical description of the model.

Reference 14 considered an empirical approach and accumulated a great deal of experimental data to develop an expression that predicted the erosion rate of 2024 aluminum alloy impacted by silicon dioxide particles for all angles of impingement. This expression is similar in form to Equation (1) for moderate-angle impacts, and also includes terms that were similar to those suggested in References 9, 10, and 11.

Reference 15 recommends a slight correction to this expression. After this correction is made, the description of erosion rates becomes

$$\varepsilon = K_1 f(\beta_i) V_i^2 \cos^2 \beta_i [1 - R_T^2] + f(V_{in}) \quad (2a)$$

where

$$R_T = 1.0 - 0.00525 V_i \sin \beta_i \quad (2b)$$

$$f(\beta_i) = [1.0 + CK(K_{12} \sin \frac{\pi}{2} \frac{\beta_i}{\beta_o})]^2 \quad (2c)$$

$$f(V_{in}) = K_3 (V_i \sin \beta_i)^4 \quad (2d)$$

$$CK = \begin{cases} 1 & \beta_i \leq 2 \beta_o \\ 0 & \beta_i < 2 \beta_o \end{cases} \quad (2e)$$

The constants K_1, K_{12}, and K_3 are related to the type of surface material and particle. Table 1 is an accumulation of the values of these constants for several different materials and types of impacting particles.

Figure 2 illustrates the rates that this equation predicts for the erosion caused by silicon dioxide particles impacting on a surface of 410 stainless steel. Similar curves would result for most other ductile surface materials. These curves illustrate the fact that the greatest amounts of erosion of ductile materials occur for impacts where the particles have moderate incidence angles with high incidence velocities. Impacts at low incidence velocities would not be expected to cause significant amounts of erosion, and impacts at high incidence angles could lead to a significant amount of erosion at high velocities.

Brittle Erosion

Reference 16 explains the phenomenon of a particle impacting on the surface of a brittle material. The phenomenon that occurs in this case is different from the erosion that occurs when the ductile material is struck by the particles.

When a brittle material is subjected to the impact of a particle, the surface near the point of contact is subjected to a very large, concentrated compressive stress. This concentrated stress causes a system of fracture cracks to radiate away from the contact point. The depth of penetration of the fracture system can be related to the stress. Finally, assuming that the material included in the crack system is lost because of erosion, a theoretical expression is developed.

This expression, which describes the volume of material removed, Q, by the impact of a particle with radius r and incidence velocity V_i, is given by

$$Q = K_4 \left(\frac{r}{0.0254}\right)^a \left(\frac{V_i}{0.3048}\right)^b \tag{3a}$$

where

$$a = \frac{3.6(n - 0.67)}{(n - 2)} \tag{3b}$$

$$b = \frac{2.4(n - 0.67)}{(n - 2)} \tag{3c}$$

$$K_4 = \frac{E^{0.8\left(\frac{n+1}{n-2}\right)} \rho_p^{1.2\left(\frac{n-0.67}{n-2}\right)}}{\sigma_o^{\frac{2n}{n-2}}} \tag{3d}$$

The symbol "n" is called the Wiebull Flow Distribution Function, and σ_o is a measure of the strength of the material. Table 2 gives the values of these terms for several types of materials.

Reference 12 demonstrates that the erosion of brittle materials is also influenced by the impingement angle; and, when this is included, erosion decreases from a maximum corresponding to particles impacting on the surface with incidence angles of 90°, as shown in Figure 3. This figure shows the erosion rates of high density alumina subjected to erosion by silicon carbide at 152 meters/second and illustrates that more erosion can be expected at the higher incidence angles.

Once again it is worth noting that Equation (3) describes the erosion when the particle is harder than the surface material. If the surface is generally harder than the particle, the surface would be much more resistant to erosion damage.

One limitation on the results that are presented here is that most of the data on erosion rates are based on tests that are done at conditions near standard temperature and pressure. Only one report, Reference 17, describes experimental data at higher temperatures. This report also contains an analytical derivation that includes the effect of surface temperature for the more moderate angle impacts, but not for higher angle impacts.

ANALYSIS

Previous work done on this research project has used an analytical model of a radial inflow turbine. Volume III[3] of this series of reports contains a detailed description of the turbine and the methods that were used to describe the gas flows through the turbine. This work also contains a study of the particle trajectories that were experienced by erosive sizes of particles in the turbine.

In this report, the hot gas turbine will be used and results on particle trajectories from the Volume III report will be recalled at the appropriate times. The inlet conditions of the hot gas were 1477.8°K and 8.55 atm. There were 29 nozzle blades, and 12 rotor blades with no splitters. The weight flowrate in the hot gas case was 0.821 kg/sec.

In order to investigate the erosion rates, it was decided to use a mixture of particle materials and sizes that would approximate SAE Standard Fine Dust. Because the erosion of each size and type of dust particle must be considered individually, all the dust was assumed to exist in discrete sizes. Table 3 compares the SAE Standard Fine Dust with the dust type that was assumed. Although iron oxide and calcium oxide are included in the definition of the dust used, the erosion caused

by these constituents was assumed to be zero because there is no data available on the erosion rates to be expected.

Montgomery and Clark[4] reported on an experimental investigation of the erosion in a radial inflow turbine subjected to continuous dust ingestion for long time periods. These authors used dust concentration levels of approximately $0.176\ gm/m^3$ for most of their work. This concentration of $0.176\ gm/m^3$ was assumed for the present work. Such a concentration corresponds to an $\alpha = 0.0143\%$, where

$$\alpha = \frac{\dot{w}_p}{\dot{w}_p + \dot{w}_g} \tag{4}$$

As reported in Reference 4, "this concentration would be visible only as a light haze in a normal size office."

In order to interpret the erosion rates physically, certain areas of the turbine internal surfaces were selected and the rate at which the surface contour would recess into the material was determined.

The method that was followed was to determine, based on the definition of the dust as given in Table 3, the portion of the total dust mass that a discrete species constituted. This portion is given the symbol, n_i, where $i = 1.20$ in this study. For example, the 3μ SiO_2 particles make up 70% x 39% of the total dust mass. Thus, $n_i = (0.70) \times (0.39) = 0.273$, indicating that 27.3% of the total particle weight is 3μ SiO_2 particles.

The total particle mass flowrate is found from the concentration. Using the definition of α, given in Equation (4), and solving for the particle mass flowrate with $\alpha = 0.0001429$, yields a particle total flowrate of 0.1173 gms/sec. With this, the mass flowrate of the individual species of the particles can be found as

$$\dot{w}_{p_i} = \dot{w}_{p_T} \cdot n_i \tag{5}$$

In addition, the number of particles of an individual species can be determined by dividing $\dot{w}_{p_i}$ by the mass of a particle of this species, m_{p_i}. Thus,

$$\dot{N}_{p_i} = \dot{w}_{p_i} / m_{p_i} \tag{6}$$

Equation (2) describes the erosion rates as particles strike a surface. The term ϵ is the mass of the surface material loss by erosion, divided by the mass of the impacting particles. This can be used to determine the volume of surface material removed, using

$$Q_i = \frac{\epsilon_i \cdot m_{p_i}}{\rho_s} \tag{7}$$

where ϵ_i represents the amount of erosion caused by an individual species.

In the present work, the erosion is assumed to occur on a finite surface segment. Therefore, the average depth of material removed over the complete surface by each impact of a particle species is

$$\Delta h_i = \frac{Q_i}{A} \tag{8}$$

This can also be expressed as the rate at which the surface contour changes by multiplying by the number of particles that strike the surface. Thus,

$$\left(\frac{\Delta h}{\Delta t}\right)_i = \frac{Q_i}{A} \cdot \dot{N}_{p_i} \cdot p_i \tag{9}$$

where p_i represents the probability teat an individual species of particle will strike the surface.

As an example, results in Volume III[3] indicated that very small particles will not tend to strike the scroll contours. Therefore, the probability of impact, p_i, for those very small particles will be zero.

It should be noted that substitution of Equaions (6) and (7) into Equation (9) results in the cancelling of the particle mass. Therefore it is not necessary to make an assumption concerning the shape of the particle.

The rate at which the surface contour changes is then assumed to be the summation of the contour changes for each species.

$$\left(\frac{\Delta h}{\Delta t}\right) = \sum_{i=1}^{20} \left(\frac{\Delta h}{\Delta t}\right)_i \tag{10}$$

Multiplying this by a specific time gives an estimate of the depth of material removed by the erosion phenomena.

RESULTS

Figure 4 shows the trajectories of particles with characteristic lengths of 30 cm in the scroll. Volume I[1] of this series of reports described the derivation and applicability of the characteristic length, which is

$$\delta = \frac{10}{3} \frac{\rho_p}{\rho_g} D_p \tag{11}$$

As was noted in the previous work, the gas density used in this expression should be the critical gas density based on the turbine inlet conditions. This characteristic length of 30 cm corresponds to silicon dioxide particle of 44 microns and alumina particles of 20 microns in the model turbine.

Figure 4 was first presented in Volume III[3] which also noted that particles smaller than this size particle do not strike the scroll contour but instead follow the gas flow into the nozzle. On the other hand, particles larger than this size particle tend to follow the same general pattern of striking the scroll contour with a large number of very low angle, low velocity impacts.

As Figure 4 indicates, these particles tend to dribble along the surface until they suddenly encounter the portion of

the scroll that is suppressed to prevent it from interfering with the scroll inlet. At this location, all the particles tend to bounce with very low velocity but more moderate angle impacts before they travel into the nozzle. Because of the concentration effect, caused by the particle impacts on the scroll, all particles with characteristic lengths greater than 30 cm will tend to strike this portion of the scroll.

In this case, the particle incidence velocity was assumed to be equivalent to the gas velocity in the scroll, 26.7 meters/sec. The incidence angle was taken as 32° for all particles. The probability p_i was assumed to be zero if the species characteristic length was less than 30, and $p_i = 1.0$ if the species characteristic length was greater than 30 cm. The erosion was assumed to occur uniformly over a surface area of 1.0 cm x 0.5 cm.

Figure 5 illustrates the approximate depths of material removal for a 410 stainless steel material eroded by the dust. The figure illustrates that after approximately 1000 hours of operation, the scroll material would be removed to a depth of approximately 1mm.

Because of the concentration of the particles with characteristic lengths of 30 cm or greater toward the outer edges of the scroll, all of these particles tend to enter the same passage of the nozzles. In the turbine used in this study, all particles with characteristic lengths of 30 and 60 cm entered passage 26. Figure 6 illustrates the trajectories that particles of these approximate sizes will follow. As indicated, most of the particles can be expected to strike the pressure surface of the blade, while some of the particles would also be expected to strike the suction surface of the blade. Review of the individual trajectories of those particles that strike the surface revealed that particles with $\delta = 30$ tended to strike the surface at velocities of about 87 m/sec. while particles with $\delta = 60$ cm tended to strike the surface with velocities of about 50 m/sec. The average impact angles for the two cases were 15° and 20°, respectively.

For this study, a segment of the pressure surface 1.0 cm long and 0.8 cm wide (the width of the blade) was selected as the

erosion study area. This segment of the surface represented approximately 30% of the blade pressure surface.

The probability of impact, p_i, was assumed to be zero when the particle's characteristic length was less than 30 cm because these smaller particles do not necessarily enter passage 26. For the cases where the species characteristic length was greater than or equal to 30, the probability of impact was taken as 30% in this study.

Figure 7 shows the anticipated erosion of this surface of blade 26 with time. The greater velocities of the particles in this region would cause a considerably greater erosion rate. In this case the surface material is 410 stainless steel.

The erosion of a titanium alloy blade is indicated in Figure 8. With this material, the erosion is greater and a blade of this material would not be expected to last as long as 410 stainless steel.

After the particles pass through the nozzles and enter the vortex-rotor tip region, most will have a tendency to strike the trailing edges of the nozzle blades. Figure 9 illustrates this type of particle motion for a particle with a characteristic length of 30 cm. As indicated in the figure, trajectories similar to these occur for particles with characteristic lengths as small as 6 cm. This corresponds to a silicon dioxide particle of 8 microns and an alumina particle of 6 microns in this turbine model.

In addition to these results, Volume III[3] also explains that smaller particles will have a tendency to move toward the nozzle blade trailing edges and that some will strike the surfaces.

Based on these results, the incidence angles were assumed to vary from 20° for particles with characteristic lengths of 3 cm to 50° for particles with characteristic lengths of 30 cm or greater. The incidence velocities were also assumed to vary from about 400 m/sec for the smaller particle to 550 m/sec for the larger particle. Results presented in Volume III indicated that larger particles have a greater tendency to enter the rotor. These particles are then struck by the rotor and accelerated to tangential velocities that are at least equal to the

rotor wheel speed. In this turbine model, the rotor tip speed is 550 m/sec.

The surface area subject ot the uniform erosion was assumed to be 1.3 cm long by 0.8 cm wide (the passage width).

The probability of impact was assumed to be a combination of several things. The probability of a particle striking the surface if it entered the passage was assumed to be 50% for particles with $\delta < 6$, and assumed to be 100% for particles with $\delta \geq 6$. This was multiplied by the reciprocal of the number of blades, reflecting the fact that the particles were assumed to be uniformly distributed throughout the flow. In this case, the number of blades was 29. Finally, the probability was multiplied by the number of times that a particle strikes the nozzle blades before it breaks apart. In this case, the number was arbitrarily assumed to be 5.

A comment should be made here that there does not seem to be any basis for the determination of the number of times the particles strike the surfaces before they break apart. A review of the literature revealed no information other than Reference 17, which contains micro-photographs of particle segments imbedded in surface material. As better data becomes available, increasing or decreasing this number will correspondingly increase or decrease the erosion rates with time.

Figure 10 shows the resulting surface contours on the stainless steel and titanium blades. The higher incidence velocities of the particles on this region of the nozzle blade have resulted in a much higher rate of erosion. The figure reveals that after only 30 minutes of dust ingestion at these concentration levels, the nozzle trailing edges have been completely remove.

The study of particles in the rotor[3] revealed that most particles are traveling relatively slowly as they enter the rotor, but are accelerated to very high velocities when the rotor overtakes the slowly moving particle and strikes it. Figure 11 illustrates the motion of particles with characteristic lengths of 15 cm as they enter the rotor. This figure

illustrates that the impact phenomenon in this case occurs with incidence angles that are quite high.

In analyzing the erosion rates, the incidence velocities were assumed to be 300 m/sec. This number was selected based on information presented in Reference 3. The incidence angles were assumed to be 90°.

In estimating the probability of impact, the fact that particles with characteristic lengths equal to 6 cm or smaller did not tend to penetrate into the rotor, was used to set $p_i = 0.0\%$ for these particle species. For larger sizes of particles, the p_i was assumed to increase uniformly up to $p_i = 50\%$ for particles with characteristic lengths of 30 cm or larger. As in the case with the nozzle trailing edges, this probability was divided by the number of rotor blades, 12, and multiplied by 5, which reflected the arbitrary assumption that the particles strike the rotor 5 times before they break apart. As explained before, there is no basis for determining an estimate of this number and the selection of 5 was completely arbitrary.

The surface area in this case was taken as 0.5 cm along the blade surface by the 0.8 cm depth of the blade channel. The erosion was assumed to occur uniformly over this surface.

Figure 12 shows the tip contours as a function of time. Both stainless steel and titanium materials are indicated. The figure shows that the rates of erosion are not as severe as those that occur on the nozzle trailing edges, but there is still a significant amount of erosion.

For comparison purposes, information on the volume removed per impact expressed in Equation (3) was used to estimate the erosion rates that would occur in the rotor tip if the rotor were constructed of harder materials. The information on this equation given in Reference 12 and 16 correspond to the erosive cutting of the surface material by silicon carbide particles. Although these particles are very much harder than the silicon dioxide particles and alumina particles used in the assumed dust, the data for the SiC particles was used because data for the other two types of particles were not available. Thus,

the results which will be presented are conservative in that they suggest greater amounts of erosion than would actually occur.

Figure 13 shows the changes to be expected in the rotor tip contour with time. As indicated, the harder, more brittle material has reduced the erosion significantly. Of special significance is the hardened steel blade that loses significant amounts of material only after very long time periods.

DISCUSSION OF RESULTS

The study of erosion with time in the portion of the scroll contour where the suppressed scroll begins revealed that the surface in this region would be removed to a depth of approximately 1 mm after 1000 hours of continuous operation. This surface erodes because even though the velocities in the scroll are relatively small, the scroll tends to push the particles into a relatively small region so that most particles strike the same area.

A comparison of this result can be made with damage to a radial turbine engine which was subjected to a slightly higher dust concentration levels for long time periods. Montgomery and Clark[4] reported that the turbine scroll on their test configuration failed after 75 hours of continuous operation. They also reported that the material was very thin around the location where the material was eroded completely through.

Because most particles of the larger sizes are forced into very small regions within the flow field, the cumulative damage is greater. This occurs on a few of the nozzle blades near the end of the inlet scroll. In the turbine model that was studied, all particles tended to enter the same nozzle blade passage, and thus the single blade would experience a greater amount of erosion damage.

In a real turbine, the damage is probably spread uniformly over two or three blade passages, and in such a case the times indicated in Figures 5 and 6 would be conservative by factors of two or three.

A more significant erosion effect has been demonstrated on the trailing edges of the nozzle blades. Particles are accelerated to quite high velocities in the vortex and rotor tip regions of the turbine, and particles of all sizes in the study indicated here would tend to cause erosion on the trailing edges of the nozzle blades. The results indicate very high rates of surface material removal. This indication agrees with the findings of Montgomery and Clark[5], who reported very severe erosion problems in this region of their turbines. These authors reported that they were required to replace this part of their turbines more often than they had anticipated.

A comment should be made that in the present study each particle was allowed to strike the nozzle blades 5 times before it was assumed that the particle broke up. Again, no data is available concerning how often the particles would, on the average, strike the surfaces before they would tend to break apart. The extremely high erosion rates on the nozzle blades indicated in this study perhaps suggest that the particles break apart quite rapidly, after only one or two impacts on the surface. Such an event would result in the indicated contours after several hours of continuous dust ingestion instead of after only 30 minutes. This is still a very short time period for such a significant amount of erosion.

Experience with the radial turbine experimental test equipment described in Volume III[3] of this series of reports indicated that as the material in the trailing edges of the nozzle blades was removed, the trailing edges became razor sharp and then curled upward into the blade passage. This would tend to cause a serious distortion of the flow through each of the nozzle passages and probably is the source of the greatest performance drop in the turbine. It is worth noting again that 410 stainless steel material seems to be slightly better in terms of erosion than the titanium alloy.

The rotor tip is subjected to a large number of normal impacts because of the way in which the tip overtakes and strikes the slower moving particles. The results in this region

of the turbine revealed that it will not lose a significant amount of material in a matter of hours. In addition, conservative estimates of the erosion rates of more brittle materials indicated that corresponding material loss from these materials would take 3 times as long for blade materials of aluminum oxide and 20 times as long for blade materials of hardened steel.

Although significantly more resistant to erosion than the more ductile materials, the materials suggested for the construction of ceramic radial turbine rotors may be much more likely to erode under the action of normal impacts. Therefore, care should be exercised in drawing conclusions that brittle materials will not erode as rapidly as the ductile materials. Data indicated in Reference 12 and 16 show that several refractory materials erode at rates more than an order of magnitude larger than the hardened steel and aluminum oxide used in this study.

Montgomery and Clark[4] reported very little erosion damage to their rotor and indicated that the changes were more in the nature of a polishing of the rotor surfaces. This could also suggest that most of the particles tend to break up after striking the nozzle blades. The smaller particles that result from this break-up would tend to move through the rotor generally following the streamlines and striking the surfaces of the rotor with very low-angle impacts.

In addition, the lack of erosion damage on the tip of their turbine could be caused by greater velocities of the particles in the rotor tip region. If the particle velocity is greater, the velocity with respect to the rotor tends to be smaller, thus significantly decreasing the amount of erosion that occurs.

Finally, it is again noted that the data on erosion rates that has been used here is data that has been accumulated at room temperature. The significantly higher temperatures in the turbine influence several areas of concern.

Equation (1) for the erosion of ductile materials at moderate incidence angles indicates that the erosion is inversely proportional to the materials' flow strength at the temperature of the material. At higher temperatures, this flow strength

will most likely be smaller, resulting in a corresponding increase in the erosion rates.

Reference 17 also contains a similar formula that relates the erosion to the reciprocal of the difference between the material melting temperature and the gas temperature. At the higher gas temperatures, the temperature difference would be smaller and the erosion rates higher.

It should also be noted that the inlet stagnation temperature of the gas is greater than the melting temperature of the silicon dioxide particles. At these high gas temperatures, this suggests that the erosion would be caused only by the alumina particles because the silicon particles would have formed droplets and be in a liquid state. Generally, this would approximately double the time required to cause the indicated amounts of erosion.

CONCLUSIONS

An analytical study of the rate at which material is removed by ingested dust from the internal surfaces of a typical radial inflow turbine has been presented.

The study indicates that there are several regions which experience very severe erosion material loss, and other regions that experience moderate levels of erosion material loss.

The greatest amount of material loss occurs in the trailing edges of the nozzle blades where very high velocity, moderate angle impacts occur. In addition, the tip region of ductile materials will also be subject to serious levels of erosion loss.

The region near the end of the scroll and a few of the nozzle blades near this location experience moderate erosion rates. This occurs even though the velocities of particles in these regions tend to be relatively slow. However, all particles tend to impact on relatively small areas and this concentration effect leads to significant amounts of erosion.

The effect of this erosion on the contours of the scroll and blade surfaces has been indicated in the form of changes in the contours with time.

REFERENCES

1. Clevenger, W.B., Jr., and Tabakoff, W., "Erosion in Radial Inflow Turbines - Volume I: Erosive Particle Trajectory Similarity," NASA CR-134589, Lewis Research Center, 1974.
2. Clevenger, W.B., Jr., and Tabakoff, W., "Erosion in Radial Inflow Turbines - Volume II: Balance of Centrifugal and Radial Drag Forces on Erosive Particles," NASA CR-134616, Lewis Research Center, 1974.
3. Clevenger, W.B., Jr., and Tabakoff, W., "Erosion in Radial Inflow Turbines - Volume III: Trajectories of Erosive Particles in Radial Inflow Turbines," NASA CR-134700, Lewis Research Center, 1974.
4. Montgomery, J.E. and Clark, J.M., Jr., "Dust Erosion Parameters for a Gas Turbine," SAE Paper No. 538, June 1962.
5. Finnie, I., "The Mechanism of Erosion of Ductile Metals," 1958 Proceedings of Applied Mechanics (ASME).
6. Finnie, I., "An Experimental Study on Erosion," Proceedings of the Society for Experimental Stress Analysis, Vol. 12, No. 2.
7. Finnie, I., "Erosion of Surface by Solid Particles," Wear, 3, 1960.
8. Stauffer, W.A., "Wear of Metals by Sand Erosion," Metals Progress, Volume 69, 1956.
9. Bitter, J.G.A., "A Study of Erosion Phenomena," Part I, Wear, 6, 1963.
10. Bitter, J.G.A., "A Study of Erosion Phenomena," Part II, Wear, 6, 1963.
11. Nelson, J.H. and Gilchrist, A., "Erosion by a Stream of Solid Particles," Wear, 11, 1968.
12. Sheldon, G.L., "Similarities and Differences in the Erosion Behavior of Materials," Journal of Basic Engineering, ASME, September 1970.
13. Grant, G., A Model to Predict Erosion in Turbomachinery Due to Solid Particles in Particulate Flow, Ph.D. Dissertation, University of Cincinnati, 1973.

14. Grant, G. and Tabakoff, W., "Erosion Prediction in Turbomachinery Due to Environmental Solid Particles," AIAA Paper No. 74-16, 1974.
15. Ball, R. and Tabakoff, W., "An Experimental Investigation of the Erosion Characteristics of 410 Stainless Steel and 6Al-4V Titanium," Report No. 73-40. Department of Aerospace Engineering, University of Cincinnati, 1973.
16. Sheldon, G.L. and Finnie, I., "The Mechanism of Material Removal in the Erosive Cutting of Brittle Materials," Journal of Engineering for Industry, ASME, November 1966.
17. Smeltzer, C.E., Bulden, M.E., McElmury, S.S., and Compton, W.A., "Mechanism of Sand and Dust Erosion in Gas Turbine Engines," USAAVLABS Technical Report 70-36, August 1970.

LIST OF SYMBOLS

A	Area - meters^2
D	Diameter - meters
E	Young's Modulus (Newtons/meter^2)
Δh	Average depth of material removed
k_o	Constant for specific erosion
m	Particle mass - kilograms
n	Wiebull Flow Distribution function
p_i	Probability of impact
Q	The volue of material removed - meters^3
r	Radius of the particle - meters
$t(\beta_i)$	Function of the incidence angle
Δt	Specific time
V	Particle's velocity - meters/second
w	Weight loss from surface
$\dot{w}$	Mass flow rate - kilogram/second

Greek Symbols

α	The ratio of mass flow rate of particles to the total mass flow rate of gas and particle mixture
β	Relative angle between particle path and specimen surface.
β_o	Angle of attack where maximum erosion occurs
δ	Characteristic length - meters
ε	Erosion per unit mass of impacting particles
ρ	Density - kilogram/meter^3
σ_o	Stress measure of the material

Subscripts

g	Gas
i	Species or incidence
o	Initial state
p	Particle
s	Solid

Table 1. Constant Values to be Used in the Prediction of Erosion as Described by Equation (2)*

Note: These numbers correspond to the use of SI units.

Material Particle/Surface		K_1 $\frac{gm/gm}{(m/sec)^2}$	K_{12}	K_3 $\frac{gm/gm}{(m/sec)^4}$
SiO_2	2024 Al	3.95×10^{-8}	0.585	6.95×10^{-13}
Al_2O_3	2024 Al	5.73×10^{-8}	0.585	1.043×10^{-12}
SiO_2	410 SS	6.53×10^{-8}	0.293	8.94×10^{-13}
Al_2O_3	410 SS	1.246×10^{-7}	0.192	2.35×10^{-12}
SiO_2	Ti-6Al-4V	5.32×10^{-8}	0.192	8.94×10^{-13}
Al_2O_3	Ti-6Al-4V	1.113×10^{-7}		2.49×10^{-12}

* Table compiles from results presented in References 14 and 15.

Table 2. Constant values to be Used in the Prediction of Erosion as Described by Equation (3)*

Material Particle/Surface		Particle Radius Exponent a	Velocity Exponent b	K_o $\frac{m^3/particle}{m^{a+b}/sec^b}$	n
SiC	Plate Glass	4.35	3.0	3980×10^{-15}	8
SiC	MgO	3.95	2.74	1390×10^{-15}	12
SiC	Al_2O_3	3.86	2.62	529×10^{-15}	14.5
SiC	Graphite	3.78	2.69	4700×10^{-15}	16.9
SiC	Hardened Steel	3.58	2.53	28.5×10^{-15}	20

* Table compiled from information presented in Reference 12.

Table 3. Composition of SAE Fine Road Dust and Dust Used in Study

SAE Fine Dust			Assumed
Material	Density gm/cc	% by wt.	% by wt.
SiO_2	2.65	67-69	70
Al_2O_3	3.99	15-17	20
Fe_2O_3	5.12	3-5	5*
CaO	2.62	2-4	5*
MgO	3.65	0.5-1.5	0
Alkalis	--	3-5	0
Igu. Loss	--	2-3	0

SAE Fine Dust		Assumed Dust	
Size Microns	% by wt.	Size Microns	% by wt.
0-5	39	3	39
5-10	18	8	18
10-20	16	15	16
20-40	18	30	18
40-80	9	60	9
80-120	0		

* Although included in composition, erosion by Fe_2O_3 and CaO was assumed zero because of lack of data on erosion rates for these materials.

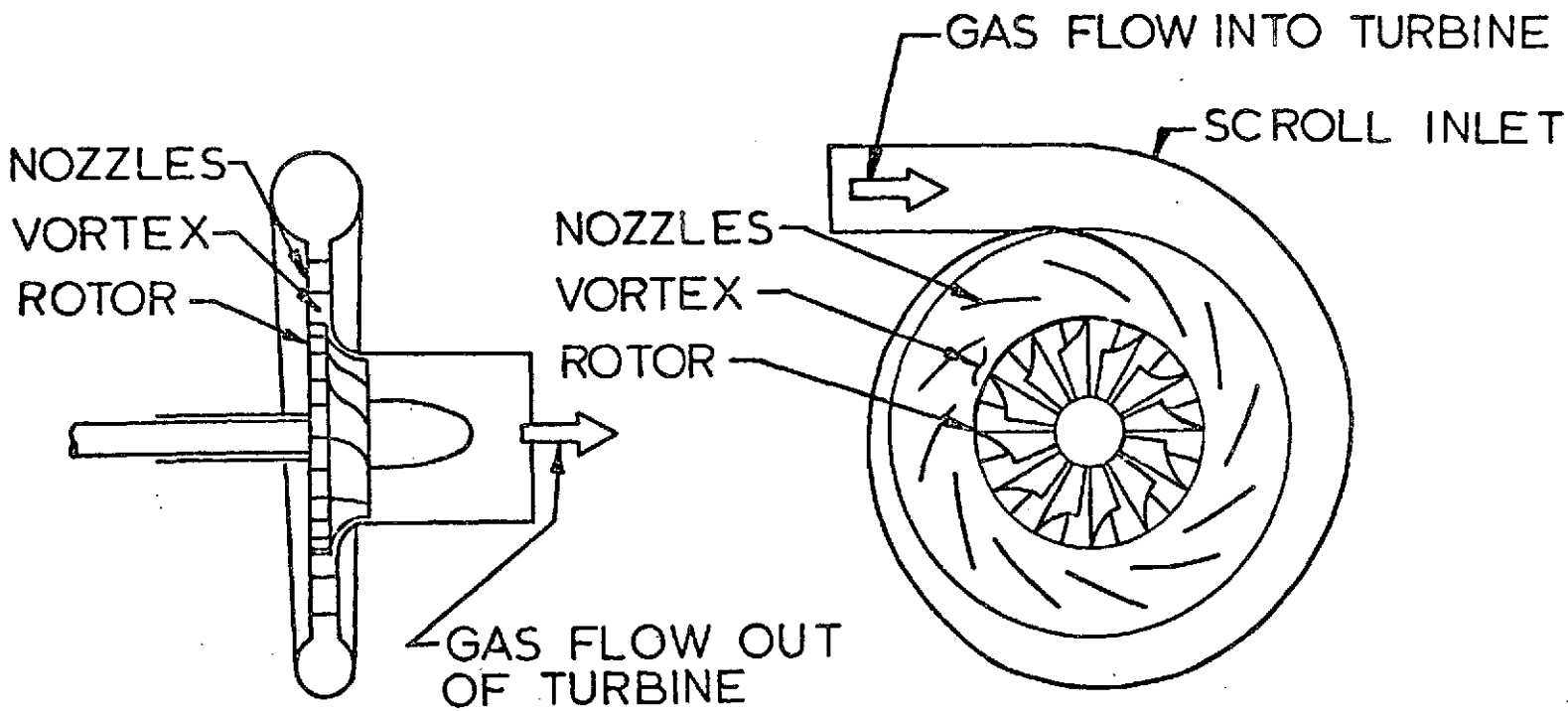

FIGURE 1. SCHEMATIC OF TYPICAL RADIAL INFLOW TURBINE.

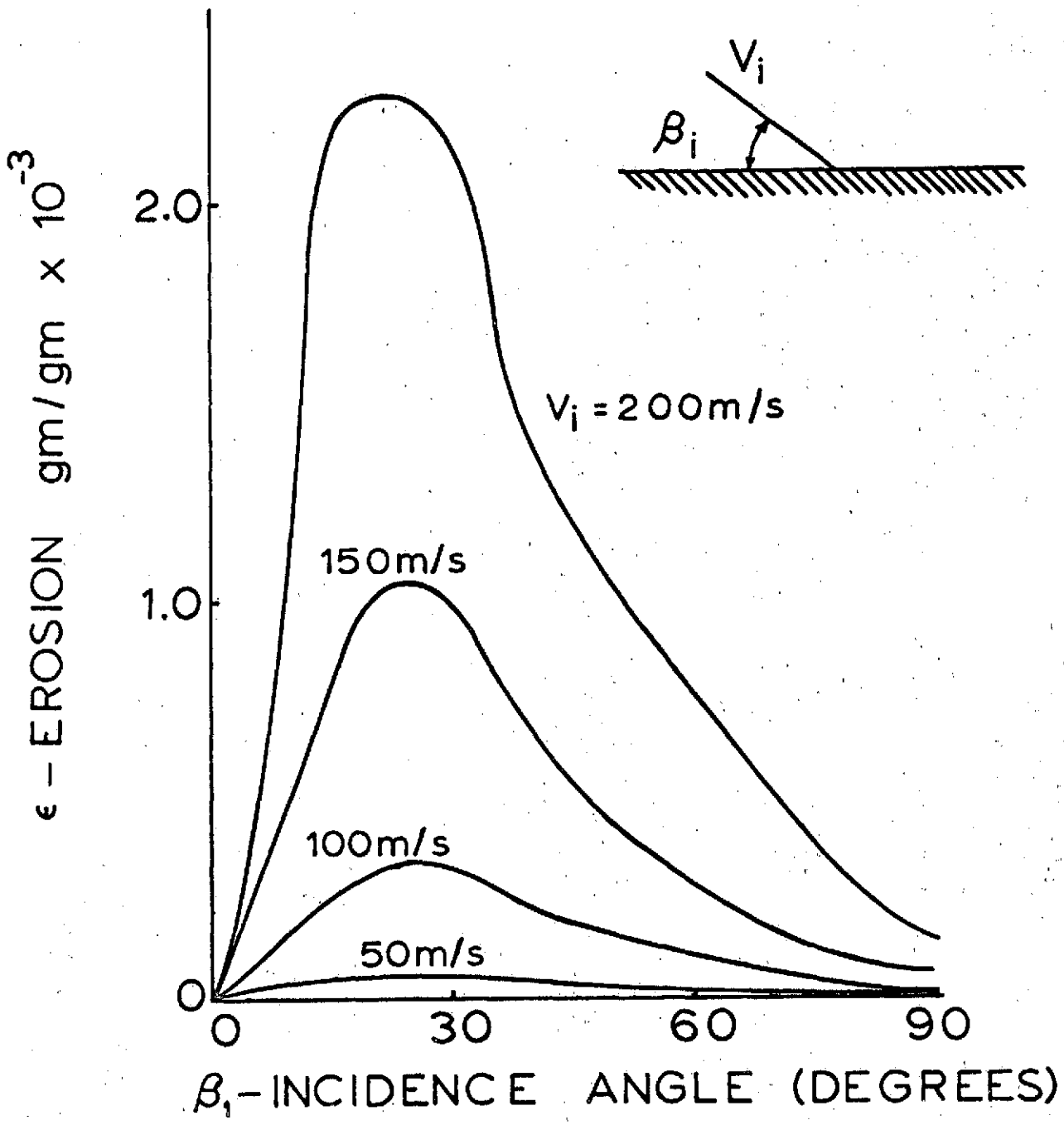

FIG. 2 EROSION AS DESCRIBED BY EQUATION 2 FOR 410 STAINLESS STEEL AND SILICONE DIOXIDE PARTICLES

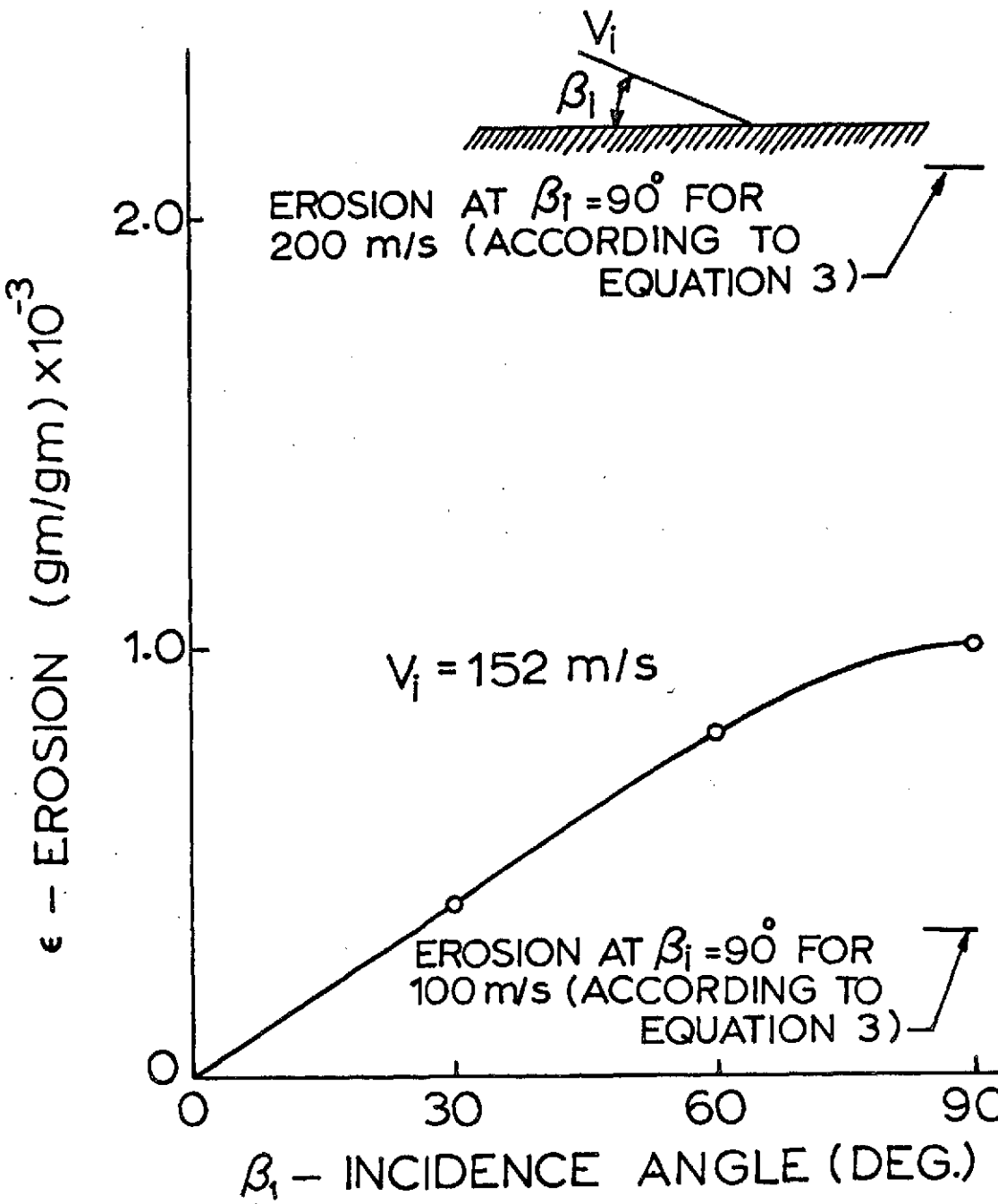

FIG. 3 EROSION OF HIGH DENSITY ALUMINA BY SILICON CARBIDE PARTICLES WITH DIAMETERS OF 127 MICRONS

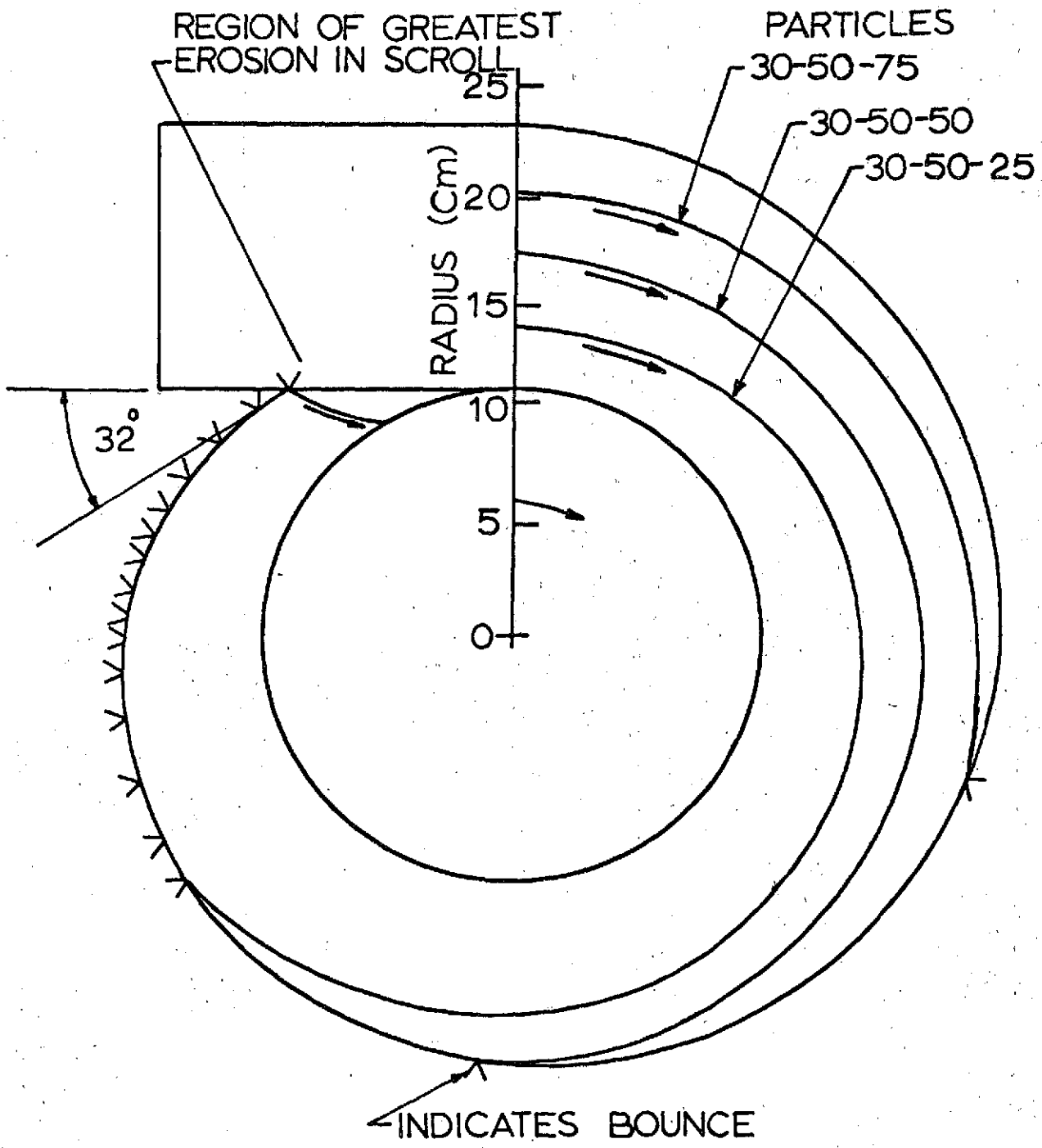

FIG. 4 TRAJECTORIES IN THE SCROLL, WITH $\delta = 30$ Cm.

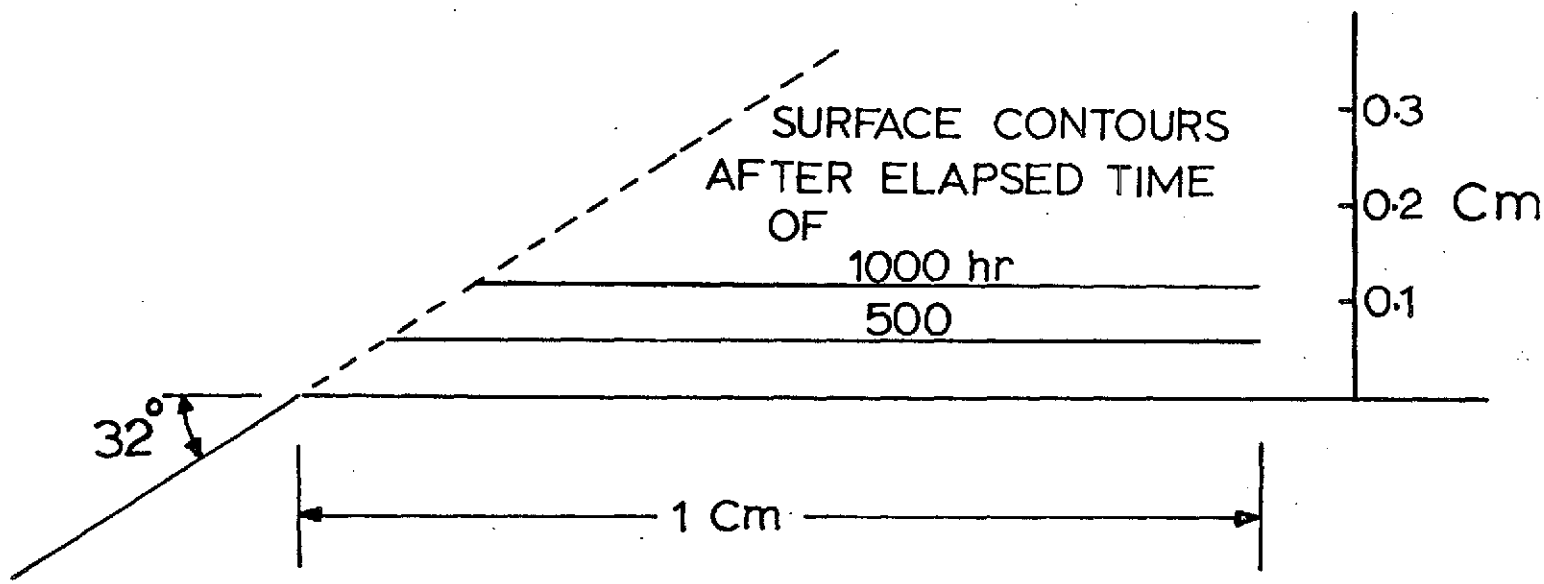

FIG. 5 DEPTH OF EROSIVE WEAR WITH TURBINE OPERATING TIME

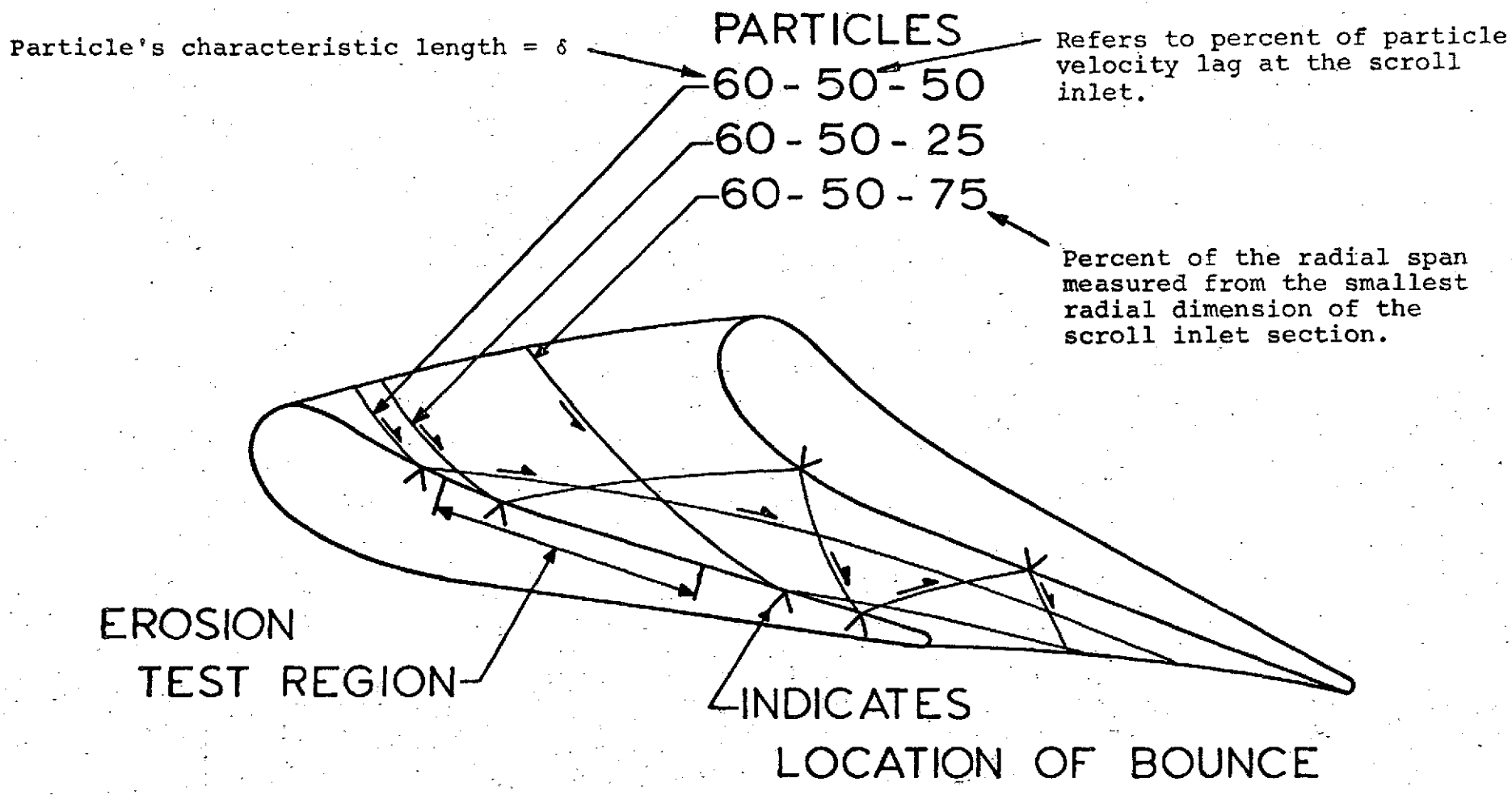

FIG. 6 TRAJECTORIES IN THE NOZZLES WITH δ = 60 cm.

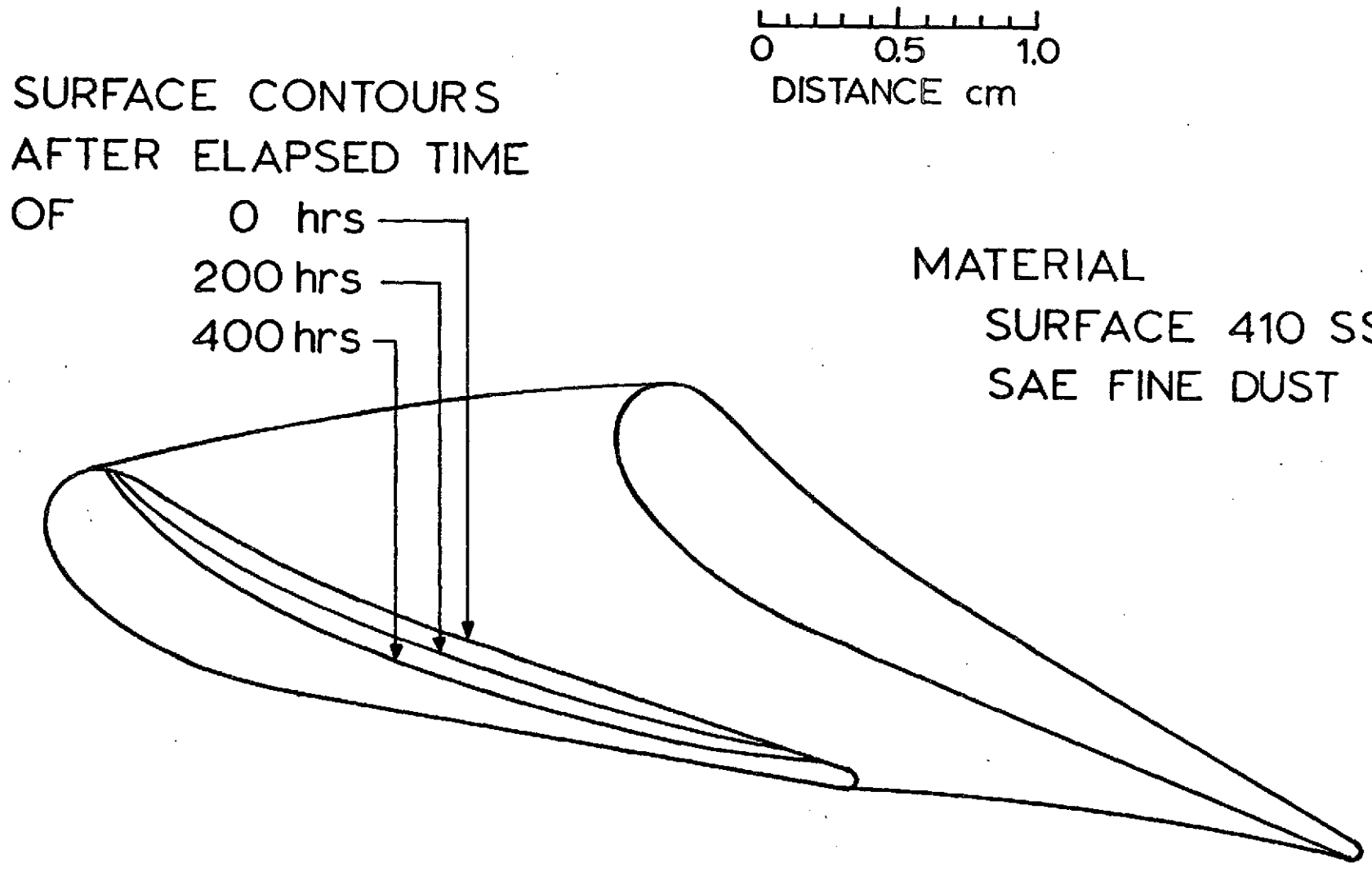

FIG. 7 EROSION ON NOZZLE BLADE 26

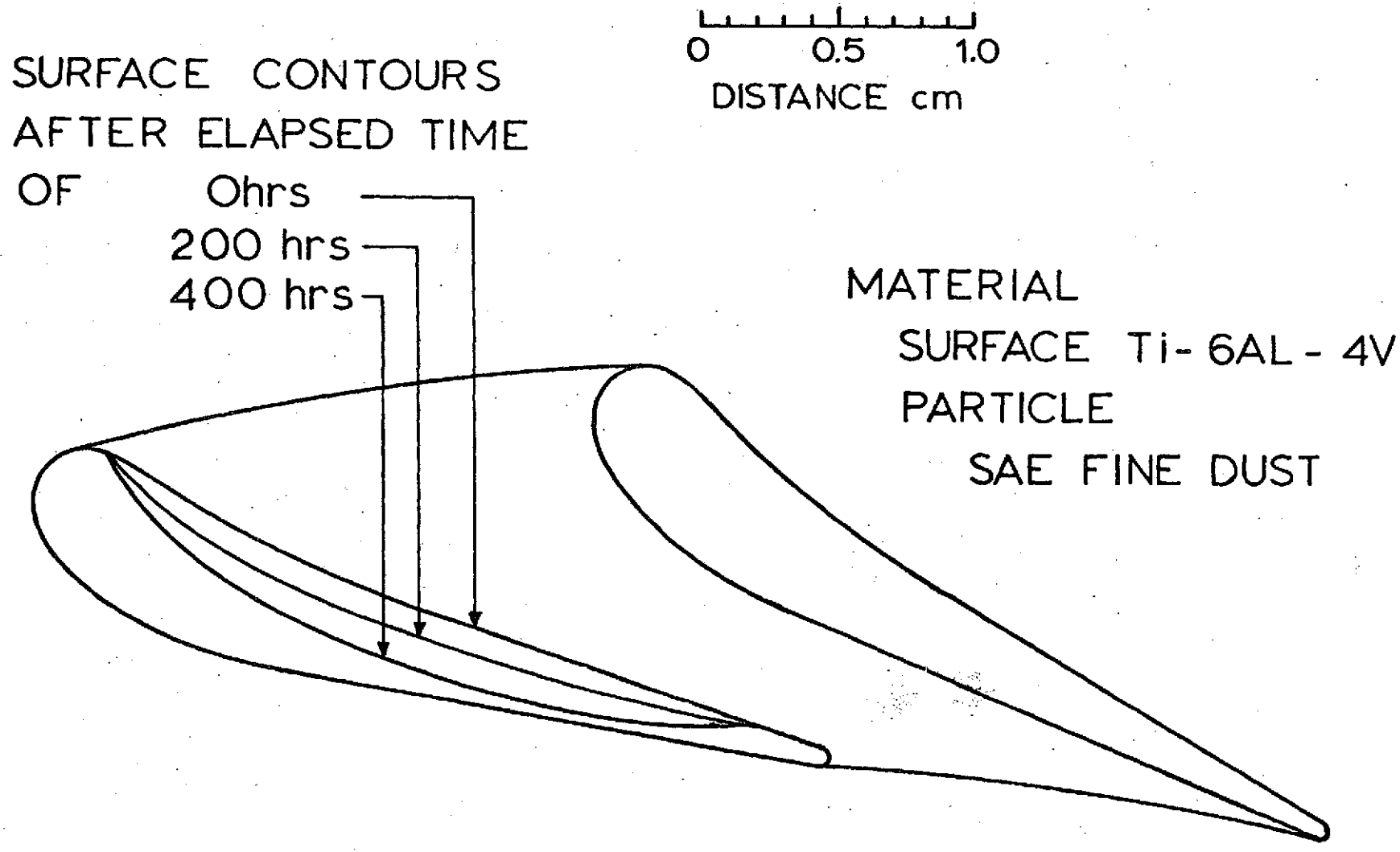

FIG. 8 EROSION ON NOZZLE BLADE 26

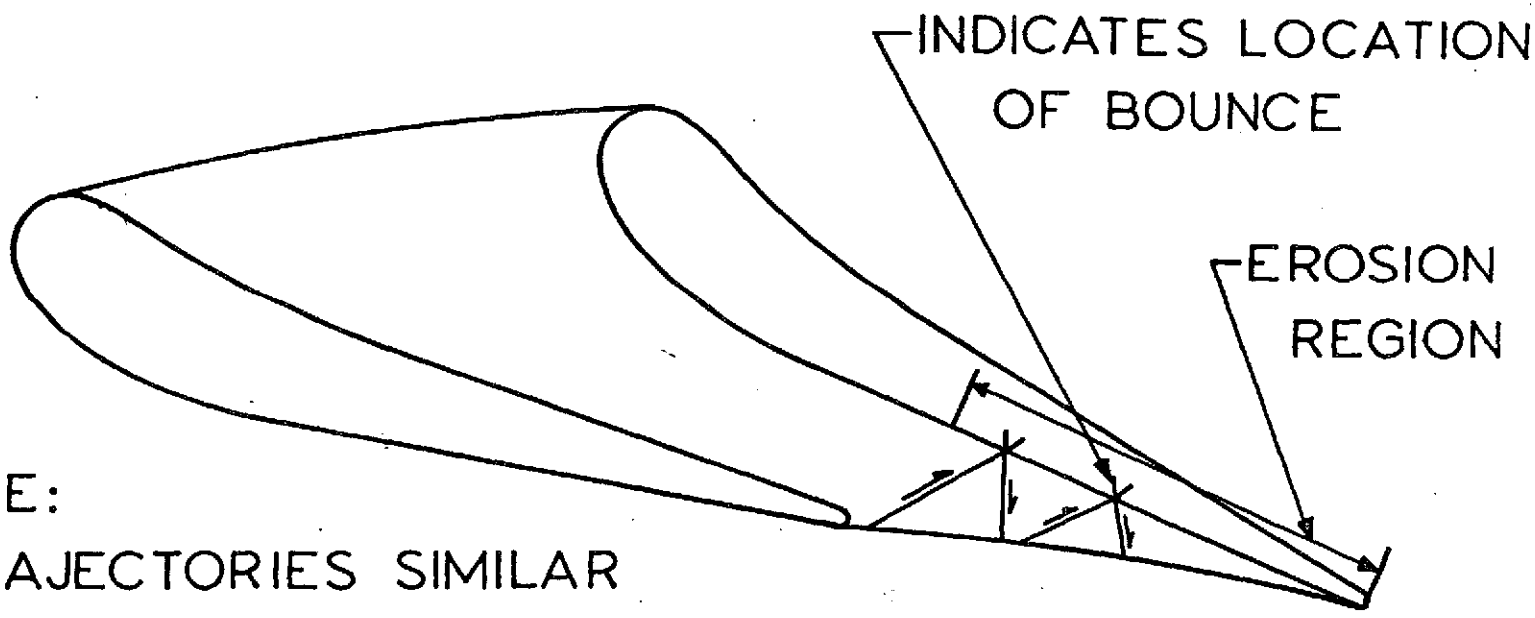

NOTE:
TRAJECTORIES SIMILAR
TO THESE OCCUR FOR δ's IN
THE RANGE $\delta > 6$ cm.

FIG. 9 TYPICAL TRAJECTORIES OF PARTICLES THAT
THAT RE-ENTER THE NOZZLES, WITH
$\delta = 30$ cm

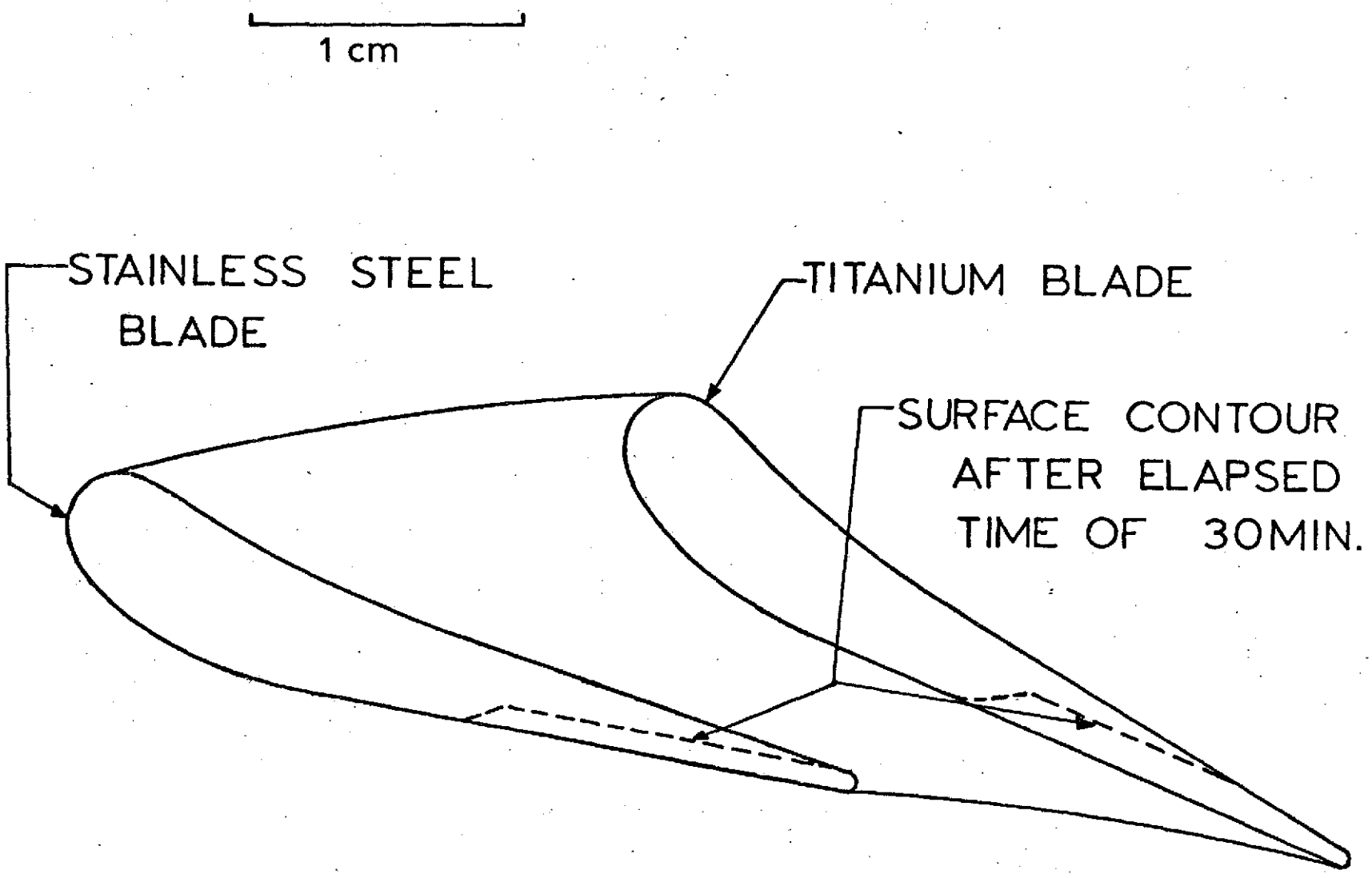

FIG. 10 EROSION OF NOZZLE BLADE TRAILING EDGES

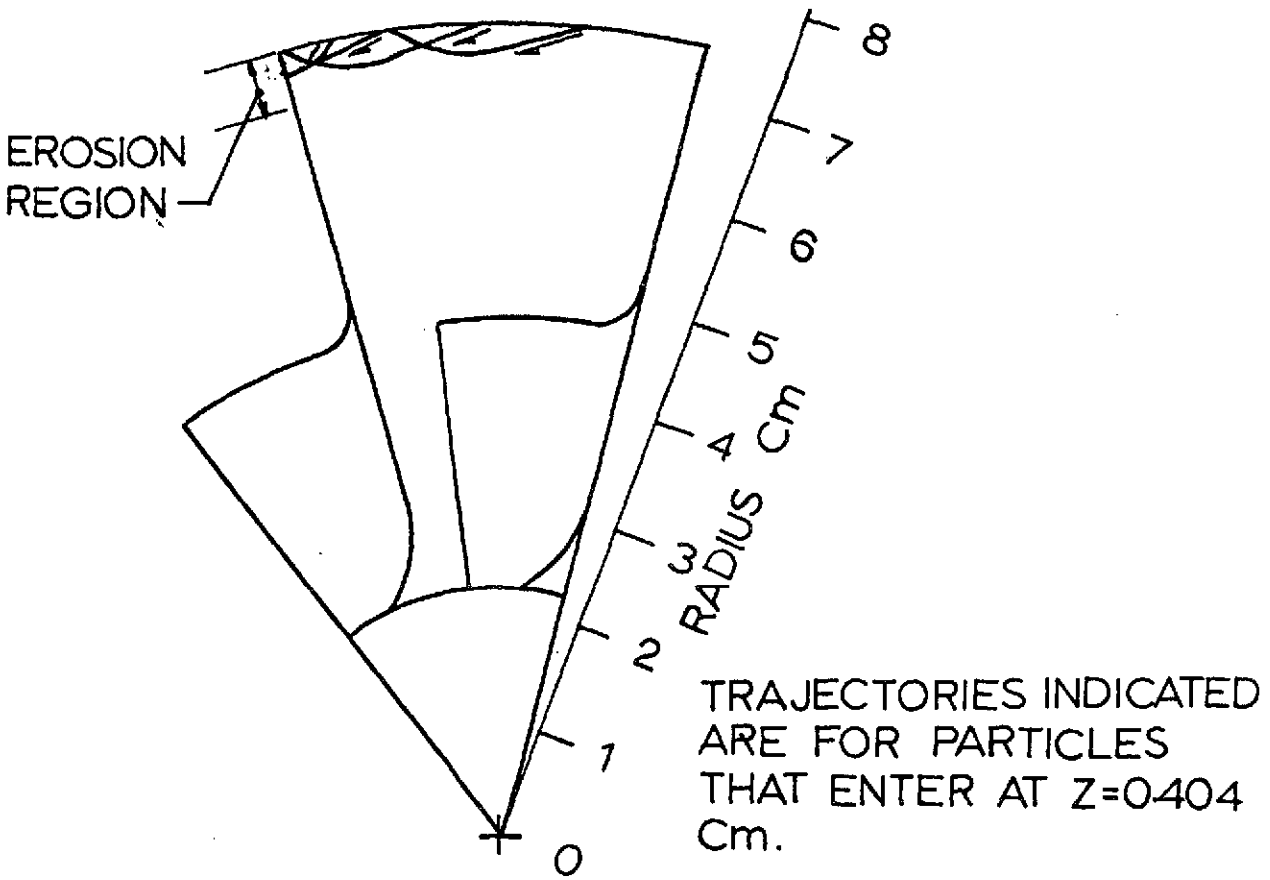

FIG. 11 AXIAL VIEW OF ROTOR WITH RESPECT TO ROTATING REFERENCE FRAME WITH δ = 15 Cm

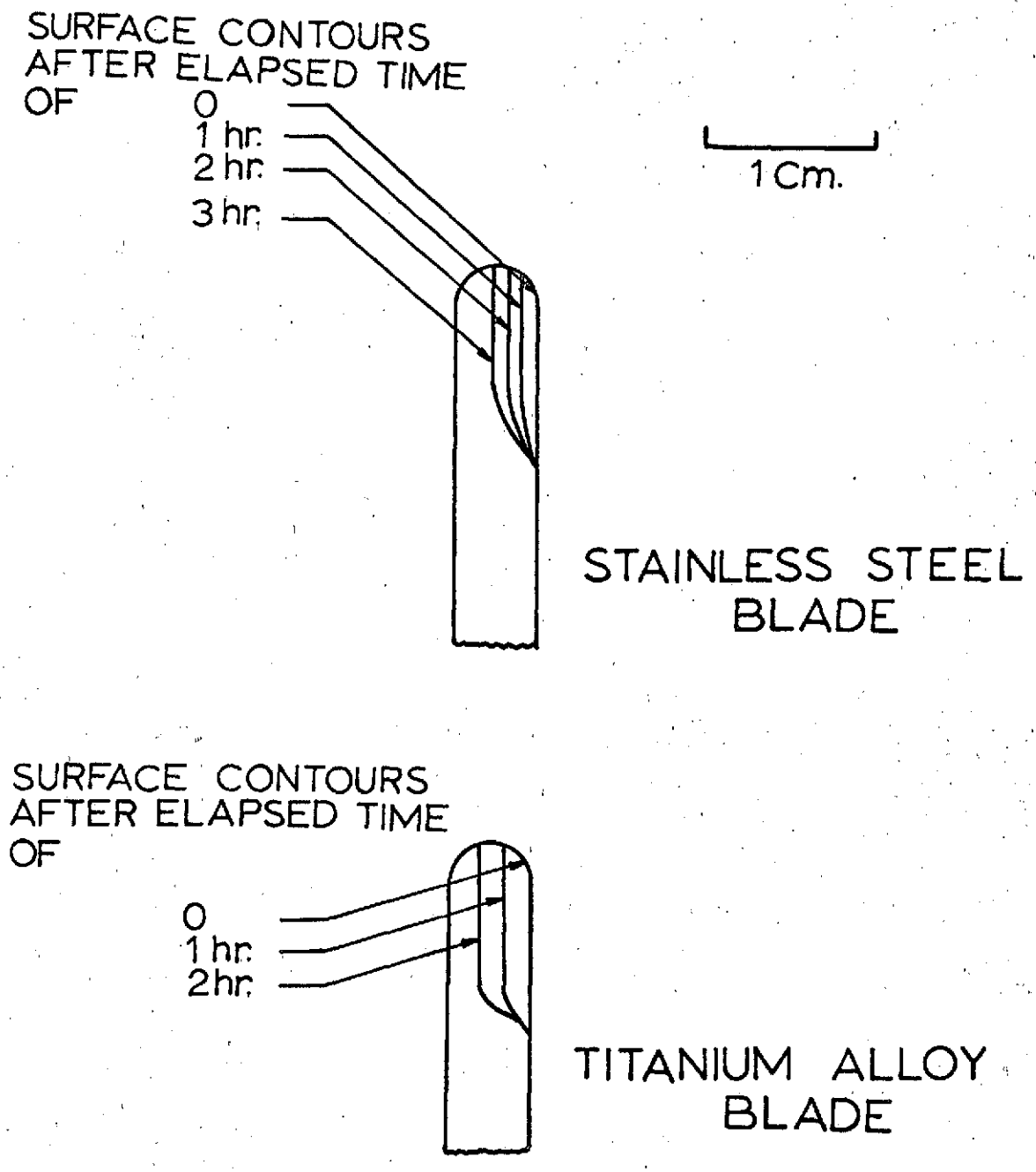

FIG. 12 EROSION SURFACE CONTOURS IN ROTOR TIP

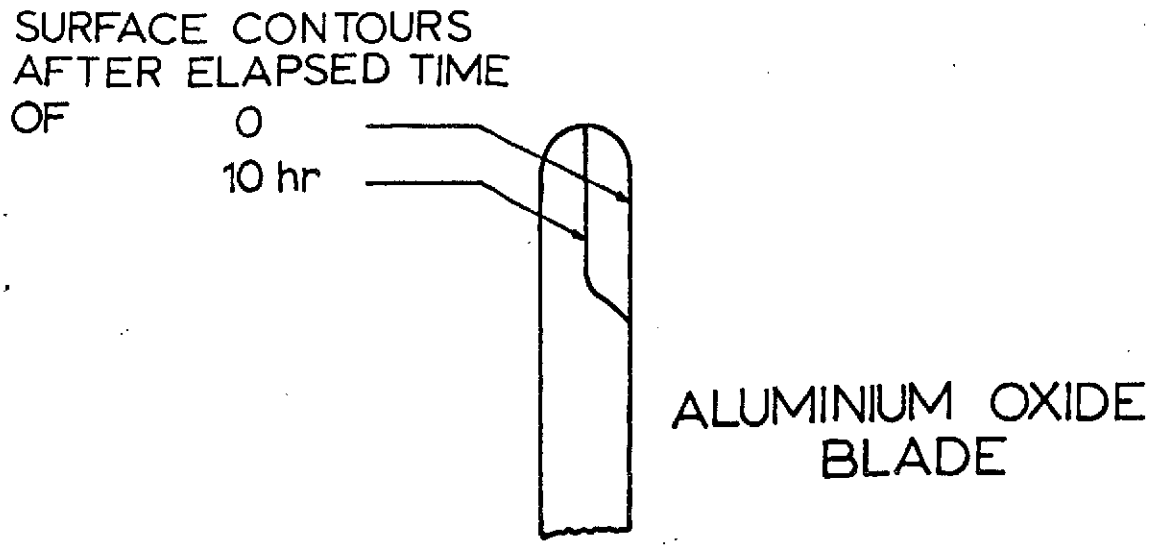

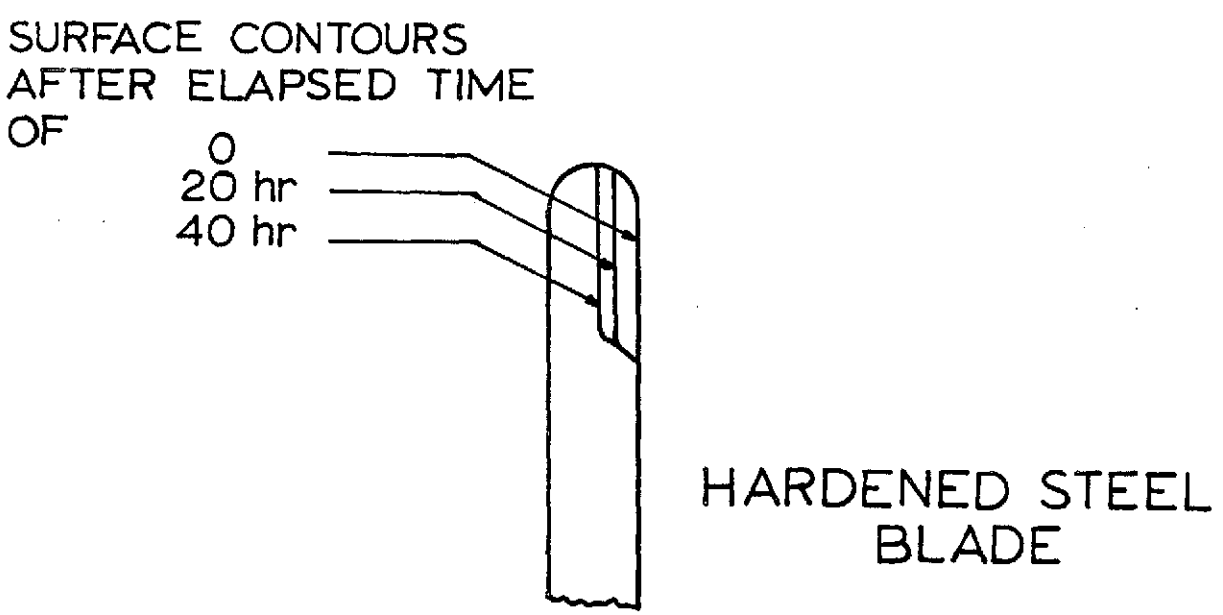

FIG. 13 EROSION SURFACE CONTOURS IN ROTOR TIP